PHYSICAL REVIEW B **80**, 085422 (2009)

Time-averaged cantilever deflection in dynamic force spectroscopy

Shigeki Kawai,* Thilo Glatzel, Sascha Koch, Bartosz Such, Alexis Baratoff, and Ernst Meyer
Department of Physics, University of Basel, Klingelbergstr. 82, 4056 Basel, Switzerland
(Received 2 June 2009; revised manuscript received 16 July 2009; published 17 August 2009)

We theoretically and experimentally study a hitherto neglected effect in dynamic force spectroscopy. The time-averaged deflection of the cantilever and the frequency shift of its second flexural mode were measured for 11 oscillation amplitudes between 12.8 and 0.51 nm above a maximum protrusion of the atomically resolved topography on KBr(001). A small but measurable time-averaged deflection was observed and the magnitude increased with decreasing amplitude. Interaction force curves essentially coincident over the whole attractive range were obtained from the measured frequency shifts with a rms noise linearly decreasing with amplitude. The correction of the tip-sample distance with the measured time-averaged deflection changes the strength of the interaction force. The deflection calculated from the extracted interaction force agrees with the direct measurement and is approximately proportional to the frequency shift except at the smallest amplitudes.

DOI: 10.1103/PhysRevB.80.085422 PACS number(s): 68.37.Ps, 34.20.Cf, 07.79.Lh

I. INTRODUCTION

Atomic scale tip-sample interactions have been independently investigated in different regimes by quasistatic[1] and dynamic force microscopy.[2] In the quasistatic contact mode, lateral variations in the total interaction force are directly detected via the deflection of the cantilever times its bending stiffness. Such measurements, however, suffer from thermal drifts and low-frequency disturbances, including mechanical vibrations, fluctuations of the optical detection system and of the light source, and noise in electronic circuit elements; the resulting sensitivity is thus low. On the other hand, after the first atomically resolved images were obtained in 1995,[3–5] dynamic force microscopy (DFM) has become a reliable technique for detecting atomic-scale short-range interactions.[6] Using an FM demodulator, the resonance frequency shift caused by interaction forces acting along the tip trajectory can be accurately measured[2] and used to control the tip-sample closest approach distance for imaging. The interpretation of such measurements can, however, be more complicated than in the quasistatic case because the mechanical oscillation of the cantilever is affected by three interrelated effects: the anharmonic distortion of the oscillation, the amplitude-dependent frequency shift, and the time-averaged deflection of the cantilever, even if interaction-induced dissipation is neglected.[7] Nevertheless, site-dependent atomic interaction forces have been successfully determined from drift-free low-temperature[8] and drift-compensated room-temperature (RT) measurements[9] of the frequency vs the displacement of the cantilever or sample holder, treating the cantilever as a weakly perturbed harmonic oscillator.[7,10] Such a treatment is justified if the interaction force is much smaller than the maximum cantilever restoring force (bending stiffness times tip oscillation amplitude).[3,10] This has led to the development of two-dimensional and three-dimensional force mappings from frequency shift vs distance measurements at different locations of the sample, so-called dynamic force spectroscopy (DFS), and to its recently implementation in homebuilt and commercial DFS software.[11–17]

So far, the influence of the time-averaged deflection in DFM has been assumed to be negligibly small or constant. One should keep in mind that, for a given tip-sample distance of closest approach, the magnitude of this deflection increases with decreasing oscillation amplitude. As a consequence, small amplitude DFM can, at least in principle, simultaneously detect the influence of interaction forces on the time-averaged deflection and on the frequency shift (i.e., a time averaged as well as a dynamic quantity). Small-amplitude DFM is anyway desirable because it allows one to optimize the signal-to-noise ratio of frequency shift measurements[18] and stable atomically resolved images have been presented under such conditions. They have been realized by using the high stiffness $k_{1st} \approx 1800$ N/m of a tuning fork[19] or the high *effective stiffness* ($k_{2nd} \approx 1500$ N/m and $k_{3rd} \approx 10\,000$ N/m) of the second or third flexural resonances of commercially available Si "noncontact" cantilevers.[20–22] The use of such higher resonances is well suited for simultaneous measurements of the time-averaged deflection and frequency shift because the static stiffness k_0 of around 30 N/m can lead to a measurable time-averaged deflection while it is still high enough to avoid the cantilever jump-to-contact instability which typically occurs with the much softer cantilevers used in contact mode.

In this paper, we theoretically and experimentally study effects of the time-averaged deflection in DFS. Force spectroscopy performed using different amplitudes on a KBr(001) sample reveals that this deflection affects quantitative determinations of the interaction force for amplitudes approaching the interaction range. A procedure to obtain amplitude-independent force vs distance characteristics is proposed and validated. It is also found that unavoidable deformations of the tip apex and, eventually, of the sample surface can significantly affect such characteristics at distances less than the interatomic spacing even if no detectable instabilities occur.

II. THEORY AND SIMULATIONS

Figure 1(a) shows a schematic drawing of the cantilever with the tip oscillating at its free end above the sample surface. The nominal tip-sample distance is determined by the

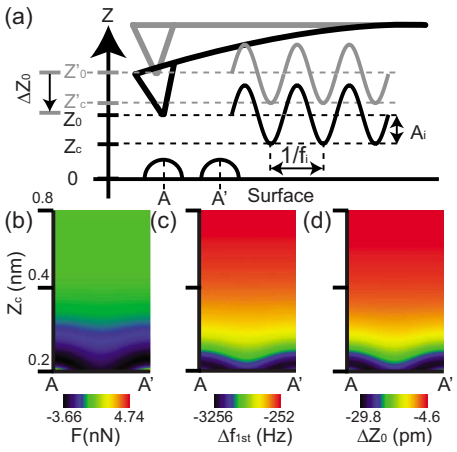

FIG. 1. (Color online) (a) Schematic drawing of a cantilever oscillating above the sample surface in the attractive range. [(b)–(d)] Calculated two-dimensional maps of (b) the interaction force, (c) the frequency shift, and (d) the time-averaged deflection. Assumed parameters: $f_{1st}=150$ kHz, $A_{1st}=1$ nm, $k_0=k_{1st}=30$ N/m, $R_{tip}=5$ nm, and $\lambda=79$ pm.

dc voltage applied to the sample Z scanner. More precisely, the controlled variable is the vertical displacement with respect to the cantilever holder or, equivalently, the equilibrium position Z_0' of the tip far from surface. However, the cantilever is statically bent by the time-averaged interaction force which causes a time-averaged deflection ΔZ_0 (negative, i.e., toward the sample if the force is attractive). The actual equilibrium position is therefore $Z_0=Z_0'+\Delta Z_0$. If higher harmonics of the oscillation are neglected, the steady-state motion of the tip apex is well described as $Z(t)=Z_0+A_i\cos(2\pi f_i t)$, where A_i and f_i are the amplitude and the resonance frequency of the self-excited ith flexural mode. The closest approach distance in each oscillation cycle is $Z_c=Z_0-A_i$. The time-averaged deflection can be obtained by Fourier transforming the equation of motion of the vibrating cantilever and evaluating the zero-frequency term, viz.,

$$k_0\Delta Z_0=\frac{1}{2\pi}\int_0^{2\pi}F(Z)d\theta=\frac{1}{\pi}\int_{-1}^{1}F(Z_0+A_iu)\frac{du}{\sqrt{1-u^2}}, \tag{1}$$

where $F(Z)$ is the conservative interaction force averaged over forward and backward swings[23] acting on the tip. A typical DFM cantilever with a static stiffness k_0 of 30 N/m would be bent 33 pm by a static interaction force of 1 nN, a small but detectable deflection, which is predicted by Eq. (1) in the limit where the amplitude becomes small compared to the interaction range λ or to Z_c, whichever is smaller (typically λ). On the other hand, the frequency shift can be obtained from the Fourier coefficient at the resonance frequency of the equivalent point-mass oscillator with the effective spring constant of the ith mode.

$$A_ik_i\frac{\Delta f_i}{f_i}=-\frac{1}{2\pi}\int_0^{2\pi}F(Z)\cos\theta d\theta$$

$$=-\frac{1}{\pi}\int_{-1}^{1}F(Z_0+A_iu)\frac{udu}{\sqrt{1-u^2}}. \tag{2}$$

For a cantilever with a uniform cross section and force applied at its free end, the equivalent oscillator has an effective spring constant $k_i\cong k_{1st}(f_i/f_{1st})^2$, where $k_{1st}\cong k_0$ within a few percent.[24,25] Equation (2) agrees with the expression first derived by Giessibl in the case $i=1$.[10,26] Because flexural resonance frequencies of conventional atomic force microscopy cantilevers are incommensurate, higher harmonics $nf_i(n>1)$ excited by force pulses exerted close to the turning point Z_c do not significantly couple to different resonances as long as they remain sharp, as under ultrahigh-vacuum (UHV) conditions. Furthermore, if $A_ik_i\gg\max|F|$, $\Delta f_i/f_i\ll 1$, and so are the $n>1$ Fourier coefficients of $Z(t)$, viz.,[7]

$$Z_n\approx -A_i\frac{1}{n^2-1}\frac{\Delta f_i}{f_i}. \tag{3}$$

If $A_i\gg Z_c$, the main contribution to the integrals in Eqs. (1) and (2) comes from the vicinity of Z_c, i.e., $u=\cos\theta\leq -1$ (Ref. 26) so that

$$k_0\Delta Z_0\approx A_ik_i\frac{\Delta f_i}{f_i}. \tag{4}$$

In the opposite limit $A_i\ll\lambda$, higher harmonics are clearly negligible and Eq. (2) yields

$$k_i\frac{\Delta f_i}{f_i}=-\frac{F'(Z_c)}{2}, \tag{5}$$

which is valid when $F'=dF/dZ\ll k_i$, whereas Eq. (2) predicts $k_0\Delta Z_0=F(Z_c)$. For intermediate values of the amplitude, the difference between Eqs. (1) and (2) comes from the extra $\cos\theta=u$ on the right-hand side (rhs) of Eq. (2) so that the time-averaged deflection decays slower with increasing distance than the force gradient but faster than the frequency shift. The time-averaged deflection should also be site dependent, in analogy to quasistatic near-contact atomically resolved imaging using an overall attractive force.[27]

For comparison with measurements ΔZ_0 must be determined as a function of the controlled distance Z_0'; thus Eq. (1) should be self-consistently solved by substituting $Z_0=Z_0'+\Delta Z_0$ in the integral on the rhs. Because the time-averaged deflection is small in practice, it is sufficient to expand the argument of F to first order in ΔZ_0. Shifting the resulting correction to the left-hand side (lhs), one obtains

$$\left[k_0-\frac{1}{\pi}\int_0^{\pi}F'(Z_0'+A_i\cos\theta)d\theta\right]\Delta Z_0$$

$$=\frac{1}{\pi}\int_0^{\pi}F(Z_0'+A_i\cos\theta)d\theta. \tag{6}$$

In the limit $A_i\ll\lambda$, this reduces to the simple result

$$[k_0 - F'(Z_0')]\Delta Z_0 = F(Z_0'), \tag{7}$$

which anticipates a jump to contact of the cantilever if the bracketed expression on the lhs would vanish. Under typical noncontact DFM conditions $F'(Z)>0$ is always much smaller than k_0 and so is the correction in question for arbitrary A_i.

In order to theoretically study the dependence of the time-averaged deflection on measurement parameters, a simple model was used to represent the tip-sample interaction. Two atoms were positioned within a distance $a=600$ pm on a flat surface as shown in Fig. 1(a). The short-range interactions between the tip apex and those closest surface atoms were described by pairwise Morse-type forces as $F_{sr}=2E_{sr}/\lambda\{\exp[-2(r-\rho)/\lambda]-\exp[-(r-\rho)/\lambda]\}$, where E_{sr} is the binding energy, λ the characteristic range, and ρ the location of the potential minimum along the apex-atom axis. The parameters ($E_{sr}=2.27$ eV, $\lambda=79$ pm, and $\rho=235.1$ pm) were taken from a fit to the first *ab initio* calculation between a Si cluster with a protruding apex atom able to form a single bond with a Si adatom on the Si(111) surface.[28] Because $a-\rho\sim 4\lambda$, ignoring more distant atoms than the two closest ones is a reasonable approximation if their two contributions are periodically repeated in adjacent unit cells. The background long-range van der Waals interaction was described as $U_{vdW}=-A_H R_{tip}/(Z+Z_{off})$, with A_H being the Hamaker constant (≈ 1 eV) for Si,[29] R_{tip} the assumed tip radius (5 nm), and Z_{off} its zero offset[30] with respect to the short-range interaction (500 pm). Figures 1(b)–1(d) show computed two-dimensional contours of the interaction force, the frequency shift, and the time-averaged deflection calculated using Eqs. (1) and (2), assuming excitation of the first flexural mode, as in conventional DFS. For $A_{1st}=1$ nm, the time-averaged deflection has a distance dependence similar to the frequency shift. For instance, the computed tip trace close to the surface at constant ($\Delta f_{1st}=-1800$ Hz) shows a topographic corrugation of 56.7 pm along A-A'.[31] The corresponding *variation* in the time-averaged deflection (0.4 pm) is negligibly small. In the case of a smaller amplitude of 0.3 nm (not shown), the variation in time-averaged deflection along A-A' is somewhat larger (1.5 pm) but still quite small compared to the same topographic corrugation of 56.7 pm which was then obtained for $\Delta f_{1st}=-5585$ Hz.[31] The relative variation in the time-averaged deflection at larger Z_c (less negative Δf_{1st}) is even smaller. Thus, if the surface topography is mapped in the constant frequency shift mode, the time-averaged deflection can be regarded as constant even for small amplitude operation. This appears consistent with Eq. (4): an oscillation amplitude as small as 0.3 nm is still large compared to the decay length λ of the short-range interaction.

A more interesting behavior is obtained in the "constant height" ($Z_c'=$const) mode, which presumably allows one to avoid crosstalk between a quantity simultaneously measured with the quantity employed for distance control by using a feedback with a slow response time (low proportional to integral gain ratio). For instance, if the initial tip height was set equal to $Z_c=300$ pm above the A site, the calculated time-averaged deflection was 25 pm. In a subsequent scan along A-A' with $Z_c'=325$ pm, the time-averaged deflection, hence Z_c, was modulated by 6.1 pm while the frequency shift was modulated by 51 Hz. The Z_c modulation causes a deviation from the desired constant height and artificially enhances the contrast of the frequency shift. For this reason the mode in question has more appropriately been called "variable deflection," particularly in the context of noncontact measurements relying on long-range electrostatic or magnetic interactions.[32]

Thus, "constant" height measurements are more affected by variations in the time-averaged deflection than constant frequency shift measurements. Operation with a large amplitude can reduce this artifact but the force detection sensitivity will then also be reduced. The increase in the time-averaged deflection for decreasing Z_c' leads to systematic deviations in force spectroscopy measurements. As can been seen in Fig. 1(d), the magnitude of the maximum time-averaged deflection was approximately 29.8 pm$\gtrsim\lambda/3$. This would cause a noticeable shift if Z_c' rather than the correct distance Z_c scale were used in the force extraction.[7] Therefore, the detection of the time-averaged deflection and the distance correction are important to improve the accuracy of DFS, especially if small amplitudes are used.

III. EXPERIMENTS

Static and dynamic force measurements were performed with our homemade UHV atomic force microscope, operating at RT.[33] The KBr(001) sample was obtained by cleaving a crystal in UHV, then annealing it to remove residual charges. A commercially available Si cantilever (Nanosensors PPP-NCL) was used as the force sensor. The integrated tip was cleaned by Ar^+ sputtering after annealing at 120 °C. The effective stiffness of the first mode k_{1st} was calibrated using the measured length and width of the cantilever and first resonance frequency $f_{1st}=167\,968$ Hz. The effective stiffness of the second mode k_{2nd} was then obtained from the relation $k_{2nd}/k_{1st}=\Delta f_{1st}/\Delta f_{2nd}\cdot f_{2nd}/f_{1st}=43.7$ obtained using simultaneous excitation of the first and second resonance modes with equal amplitudes ($A_{1st}=A_{2nd}=10$ nm).[34] This procedure ensures that the offset of the tip from the cantilever end is taken into account. The time-averaged deflection was detected via the low-pass filtered optical deflection signal. The vertical deflection sensitivity was calibrated using an independent static indentation of the sample into the range where the deflection becomes dominated by the cantilever stiffness so that the signal varies linearly with the static piezo displacement. In this process, the tip was presumably terminated by a KBr cluster upon retraction.[35] For the DFM and DFS measurements, the interactions are detected with the second mode alone and each oscillation amplitude was preset using an automatic gain controller.[2] The shifted resonance frequency of the second mode was demodulated with a phase-locked loop (PLL) circuit (Nanonis Dual-OC4) which also generated the excitation signal.[36,37] The results were analyzed using the WSxM software.[38]

Figure 2(a) shows a series of frequency shift vs distance curves obtained with 11 different amplitudes from 12.8 to 0.51 nm. As discussed below in connection with Fig. 3(a), the origin of each curve was adjusted so that all converted

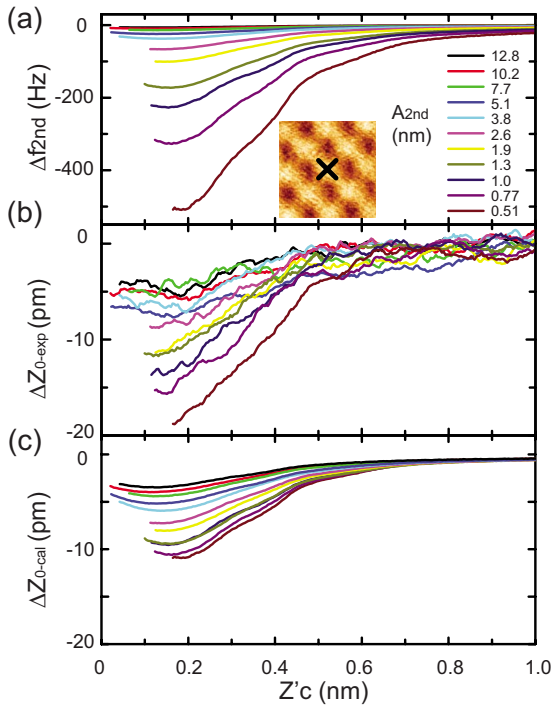

FIG. 2. (Color online) (a) A series of frequency shift curves vs nominal distance measured using 11 different amplitudes of the second flexural mode on a KBr(001) surface. The inset image was obtained with $\Delta f_{2nd}=-3.6$ Hz and $A_{2nd}=12.8$ nm. (b) Simultaneously recorded time-averaged deflection curves. Cantilever parameters; $f_{2nd}=1\ 039\ 369$ Hz, $k_0=33$ N/m, $k_{2nd}=1442$ N/m, and $Q_{2nd}=11\ 727$. (c) Time-averaged deflection curves estimated from the measured frequency shift using Eq. (4).

force curves match at one position. The DFS measurements were performed above the maximum marked in the image shown in the inset, keeping the sample properly positioned by means of an atom-tracking software (Nanonis SPMCS-AT4). In such measurements, a phase error $\Delta\phi_{err}$ due to the finite response time of the PLL demodulator causes a spurious deviation $[\approx -f_i/2Q_i \tan(\Delta\phi_{err}/2)]$ in Δf_i.[39] With a small amplitude, a relatively large frequency shift is caused at short distances, as implied by Eq. (2). A wide bandwidth of the PLL demodulator must be therefore be set to follow the large frequency change; this implies in turn a noisy output signal. At RT, setting a slow sweep of the sample Z scanner to

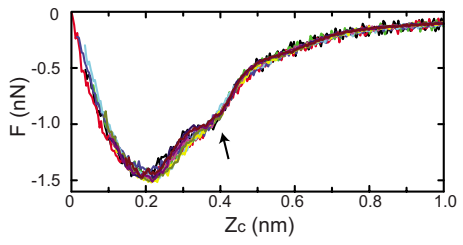

FIG. 3. (Color online) Essentially unique conservative interaction force extracted from frequency shifts measured with 11 different amplitudes plotted against the corrected tip-sample distance Z_c. The colors, one for each amplitude, are the same as in Fig. 2(a). The Z_c scale is adjusted so that all curves match at $Z_c=0.44$ nm and that $F\approx 0$ at $Z_c=0$.

reduce this noise is undesirable because of unavoidable thermal drifts. Using the second resonance mode is more appropriate because its high stiffness reduces the frequency shift by a factor $\approx f_{2nd}/f_{1st}\cdot k_{1st}/k_{2nd}\approx 6$. A small maximum phase error of 2.3° was observed in the measurement with $A_{2nd}=0.51$ nm at $Z_c'=0.255$ nm ($\Delta f_{2nd}=-441$ Hz) and the corresponding error in Δf_{2nd} was negligibly small (0.87 Hz).

As Eq. (1) implies, the usage of a particular resonance mode does not affect the determination of the time-averaged deflection. Short- and long-range distance-dependent contributions were separately measured using sweeps of 1.0 and 32.4 nm in steps of 3.9 and 31 pm above the same site, respectively. The contact potential difference[40] was not compensated but the sweep of 32.4 nm was long enough to define a reliable zero force point. In order to further reduce the noise at short distances, a smoother short-range curve was generated by averaging over 20 successive approach-return cycles.

Figure 2(b) shows the resulting time-averaged deflection curves simultaneously recorded with the frequency shifts shown in Fig. 2(a). To clearly reveal the small time-averaged deflection, the curves were also smoothed *a posteriori*. As expected, the cantilever was statically bent toward to the surface in the attractive regime covered here. In the measurement with a large amplitude of 12.8 nm, the maximum time-averaged deflection was tiny (≅4 pm) but increased to 20 pm at the smallest amplitude of 0.51 nm. Some of those curves show minima and their position ($Z_c'\approx 0.2$ nm) move closer to the surface with increasing amplitude, just like for the frequency shifts. This is consistent with Eqs. (1) and (2). Finally, Fig. 2(c) shows the time-averaged deflection curves estimated from the measured frequency shift using Eq. (4). For large amplitudes, the calculated deflections almost coincide with the measured ones but deviate for smaller amplitude. This is consistent with the requirement $A_i < Z_c$ for the validity of Eq. (4).

IV. CORRECT FORCE VS DISTANCE AND DISCUSSION

To our knowledge, force extractions have up to now been performed from measured frequency shifts as a function of Z_c'. As mentioned in Sec. II, in order to obtain the correct dependence of the interaction force on the tip-sample distance, Z_c should actually be used for force extraction instead of $Z_c=Z_c'+\Delta Z_0$. Figure 3 shows $F(Z_c)$ curves extracted using Sader and Jarvis's algorithm[41] from the measured Δf_{2nd} curves shown in Fig. 2(a). Although a large range of amplitudes from 12.8 to 0.51 nm were used, all force curves essentially coincide, like in similar measurements on Si(111) -7×7.[13] In particular, a high reproducibility is obtained in the range $Z_c>0.4$ nm. Around −1.0 nN, a wiggle is observed in almost all curves. As suggested by atomistic simulations[15,35,42,43] assuming sharp model tips, this nonmonotonic behavior can rise at the site in question because short-range attraction between the closest tip and sample ions with opposite charges turns into repulsion with decreasing distance while the total force remains attractive. KBr being a soft material, it is not surprising that such displacements can arise. Unfortunately such displacements are not

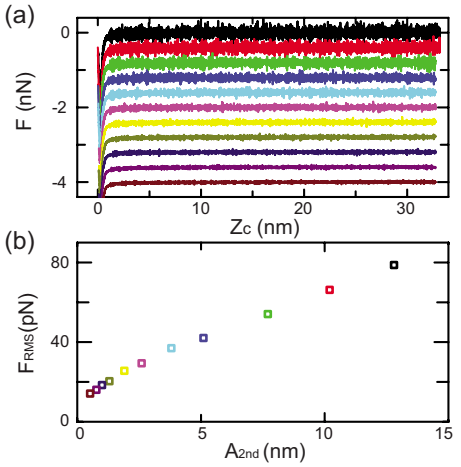

FIG. 4. (Color online) (a) Long-range force curves, each offset by 0.4 nN for clarity. (b) Rms force noise in the same range, decreasing linearly with the amplitude. The colors, one for each amplitude, are the same as in Fig. 2(a).

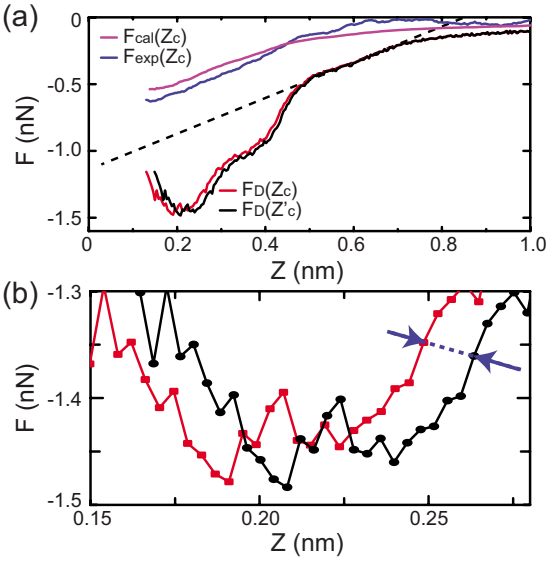

FIG. 5. (Color online) (a) Comparison of the extracted and time-averaged forces measured with the smallest amplitude of 0.51 nm. $F_D(Z_c)$ and $F_D(Z_c')$ denote the extracted force curves with and without correction for the time-averaged deflection. $F_{s\text{-}cal}$ and $F_{s\text{-}exp}$ denote the time-averaged force calculated from the extracted force using Eq. (1) and from the measured time-averaged deflection, namely, $k_0\Delta Z_0$. (b) Magnification of $F_D(Z_c)$ and $F_D(Z_c')$ in the most attractive force region.

measurable and only the nominal tip-sample distance corrected for the time-averaged deflection can be determined from experiments. Keeping in mind the likelihood of appreciable displacements at short distances, it is quite remarkable that the extracted force appears to be unique all the way to the point $F=0$ where attraction and repulsion balance.

As expected from Eqs. (1) and (2), the difference between the distance dependencies apparent in Figs. 2(b) and 2(c) becomes appreciable if Z_0 and the peak-to-peak amplitude $2A_i$ become comparable to the full width at half minimum of the attractive force well. Note that on the high Z side, this width is mainly determined by the long-range force.

Attempts to use amplitudes below 0.51 nm at short closest approach distances led to significant deviations and to steep changes in the recorded averaged frequency shifts and extracted forces. This phenomenon, which depends on the particular tip used, is under investigation.

A force sensitivity as a function of amplitude was evaluated as follows. Each single long-range force measurement [Fig. 4(a)] was fitted using the Hamaker expression for a spherical cap against a flat surface.[29] The remaining root-mean-square deviations F_{rms} are shown in Fig. 4(b): F_{rms} decreases essentially linearly with the amplitude and reaches 14 pN for the smallest one (0.51 nm). Hence, small amplitude operation is experimentally confirmed to be effective not only for imaging[44] but also for force spectroscopy.

In order to highlight the influence of the time-averaged deflection in force spectroscopy, the force was extracted with and without taking the time-averaged deflection into account for the smallest amplitude of 0.51 nm. As shown in Fig. 5(a), a shift of the curve toward smaller Z due to the time-averaged deflection can be clearly identified in the vicinity of the attractive minimum. A small vertical shift of ≈ 13 pN in the corrected force curve is also observed [arrow in Fig. 5(b)]. One may view these deviations as negligible but a systematic deviation could arise after subtracting a long-range force fit in order to obtain the short-range contribution[29] because the time-averaged deflection can become significant at close approach. Atomistic simulations[35,42,43] have shown that shifts of the distance between the closest atoms or ions can be much larger than the maximum time-average deflection detected in our experiments. The underlining ionic displacements are stronger near the tip apex. However, these phenomena arise in addition to the time-averaged deflection and it is not possible to empirically determine such displacements because the local stiffnesses of individual atoms and even the tip apex are not known. Although not measurable, such displacements can cause telltale distortions of the extracted short-range interaction force like the wiggle apparent in Fig. 3(a). At large distances, force extraction of the long-range interaction using Z_c' is sufficient.

The time-averaged force can be obtained from the measured time-averaged deflection $F_{exp}=k_0\Delta Z_0$ and compared to F_{cal} calculated from the extracted interaction force using Eq. (1). However, the sensitivity of the time-averaged deflection is so low that the results have to be smoothed. The two curves show a similar Z_c dependence with a deviation of around 20% at $Z_c=0.20$ nm. In this comparison, the calibration error of the stiffness k_0 has no effect because both force values depend linearly on k_{1st}, respectively, and because k_{1st}/k_0 is constant for a given cantilever.[24,25] The amplitude calibration is probably not the main cause of the deviation because amplitudes were precisely calibrated by the "constant γ method."[45] Furthermore, the best force fit curves shown in Fig. 3 was obtained by recalibrating each amplitude using 5% steps. The observed deviations are most likely due to the calibration of the time-averaged deflection sensitivity.

V. CONCLUSIONS

In this study, we theoretically and experimentally analyzed the time-averaged cantilever deflection in dynamic force spectroscopy with a Si cantilever on a KBr(001) sample. Narrow band self-excitation and FM detection of the shifted second flexural resonance enabled accurate measurements using several tip oscillation amplitudes down to 0.51 nm. The magnitude of the time-averaged deflection increases with decreasing amplitude. Because the smallest peak-to-peak oscillation amplitude was still larger than the full width at half minimum of the attractive force well, the maximum measured deflection is still smaller than the static deflection of the cantilever at the same distance of closest approach. Essentially coincident interaction force curves were extracted from the frequency shifts measured with various amplitudes as a function of the corrected tip-sample distance. They all exhibit a wiggle attributed to displacements of strongly interacting atoms at close approach seen in atomistic simulations. The correction due to the time-averaged deflection causes small but measurable deviations not only in the tip-sample distance but also in the strength of the extracted interaction force. The time-averaged deflection calculated from the converted interaction force coincides with its direct measurement within 20%, which is reasonable in view of the small signal and plausible calibration errors.

ACKNOWLEDGMENTS

This work was supported in part by the Swiss National Science Foundation, the ESF EUROCORE program FANAS and by the NCCR "Nanoscale Science" of the Swiss National Science Foundation.

*shigeki.kawai@unibas.ch

[1] G. Binnig, C. F. Quate, and C. Gerber, Phys. Rev. Lett. **56**, 930 (1986).
[2] T. R. Albrecht, P. Grütter, D. Horne, and D. Rugar, J. Appl. Phys. **69**, 668 (1991).
[3] F. J. Giessibl, Science **267**, 68 (1995).
[4] S. Kitamura and M. Iwasaki, Jpn. J. Appl. Phys., Part 2 **34**, L145 (1995).
[5] H. Ueyama, M. Ohta, Y. Sugawara, and S. Morita, Jpn. J. Appl. Phys., Part 2 **34**, L1086 (1995).
[6] S. Morita, R. Wiesendanger, and E. Meyer, *Noncontact Atomic Force Microscopy* (Springer, Berlin, 2002).
[7] U. Dürig, Appl. Phys. Lett. **75**, 433 (1999).
[8] M. A. Lantz, H. J. Hug, R. Hoffmann, P. J. A. van Schendel, P. Kappenberger, S. Martin, A. Baratoff, and H. J. Güntherodt, Science **291**, 2580 (2001).
[9] Y. Sugimoto, P. Pou, M. Abe, P. Jelinek, R. Pérez, S. Morita, and O. Custance, Nature (London) **446**, 64 (2007).
[10] F. J. Giessibl, Phys. Rev. B **56**, 16010 (1997).
[11] A. Schwarz, H. Hölscher, S. M. Langkat, and R. Wiesendanger, in *Scanning Tunneling Microscopy/Spectroscopy and Related Techniques*, edited by P. M. Koenraad and M. Kemerink, AIP Conf. Proc. No. 696 (AIP, New York, 2003), p. 68.
[12] A. Schirmeisen, D. Weiner, and H. Fuchs, Phys. Rev. Lett. **97**, 136101 (2006).
[13] Y. Sugimoto, T. Namikawa, K. Miki, M. Abe, and S. Morita, Phys. Rev. B **77**, 195424 (2008).
[14] M. Ternes, C. P. Lutz, C. F. Hirjibehedin, F. J. Giessibl, and A. J. Heinrich, Science **319**, 1066 (2008).
[15] K. Ruschmeier, A. Schirmeisen, and R. Hoffmann, Phys. Rev. Lett. **101**, 156102 (2008).
[16] M. Ashino, D. Obergfell, M. Haluka, S. Yang, A. N. Khlobystov, S. Roth, and R. Wiesendanger, Nat. Nanotechnol. **3**, 337 (2008).
[17] B. J. Albers, T. C. Schwendemann, M. Z. Baykara, N. Pilet, M. Liebmann, E. I. Altman, and U. D. Schwarz, Nat. Nanotechnol. **4**, 307 (2009).
[18] F. J. Giessibl, H. Bielefeldt, S. Hembacher, and J. Mannhart, Appl. Surf. Sci. **140**, 352 (1999).
[19] F. J. Giessibl, Appl. Phys. Lett. **73**, 3956 (1998).
[20] S. Kawai, S. Kitamura, D. Kobayashi, S. Meguro, and H. Kawakatsu, Appl. Phys. Lett. **86**, 193107 (2005).
[21] S. Kawai and H. Kawakatsu, Appl. Phys. Lett. **88**, 133103 (2006).
[22] S. Kawai and H. Kawakatsu, Phys. Rev. B **79**, 115440 (2009).
[23] H. Hölscher, B. Gotsmann, W. Allers, U. D. Schwarz, H. Fuchs, and R. Wiesendanger, Phys. Rev. B **64**, 075402 (2001).
[24] U. Rabe, K. Janser, and W. Arnold, Rev. Sci. Instrum. **67**, 3281 (1996).
[25] J. Melcher, S. Hu, and A. Raman, Appl. Phys. Lett. **91**, 053101 (2007).
[26] F. J. Giessibl and H. Bielefeldt, Phys. Rev. B **61**, 9968 (2000).
[27] F. Ohnesorge and G. Binnig, Science **260**, 1451 (1993).
[28] R. Pérez, I. Štich, M. C. Payne, and K. Terakura, Phys. Rev. B **58**, 10835 (1998).
[29] J. Israelachvili, *Intermolecular and Surface Forces*, 2nd ed. (Academic, London, 1991).
[30] M. Guggisberg, M. Bammerlin, C. Loppacher, O. Pfeiffer, A. Abdurixit, V. Barwich, R. Bennewitz, A. Baratoff, E. Meyer, and H. J. Güntherodt, Phys. Rev. B **61**, 11151 (2000).
[31] In practice stable imaging at such a distance would likely be prevented by atoms jumping to or from the sample. Such instabilities are not taken into account in the present simple model. And so are also precursor displacements of strongly interacting atoms which cause an enhancement of the topographic corrugation (and of the time-averaged deflection) at short closest approach distances in actual experiments and in atomistic simulations.
[32] H. J. Hug, B. Stiefel, P. J. A. van Schendel, A. Moser, S. Martin, and H.-J. Güntherodt, Rev. Sci. Instrum. **70**, 3625 (1999).
[33] L. Howald, E. Meyer, R. Lüthi, H. Haefke, R. Overney, H. Rudin, and H. J. Güntherodt, Appl. Phys. Lett. **63**, 117 (1993).
[34] S. Kawai, T. Glatzel, S. Koch, B. Such, A. Baratoff, and E. Meyer (unpublished).
[35] R. Hoffmann, L. N. Kantorovich, A. Baratoff, H. J. Hug, and H. J. Güntherodt, Phys. Rev. Lett. **92**, 146103 (2004).
[36] U. Dürig, H. R. Steinauer, and N. Blanc, J. Appl. Phys. **82**, 3641 (1997).
[37] C. Loppacher, M. Bammerlin, F. Battiston, M. Guggisberg, D.

Müller, H. R. Hidber, R. Lüthi, E. Meyer, and H. J. Güntherodt, Appl. Phys. A: Mater. Sci. Process. **66**, S215 (1998).
[38] I. Horcas, R. Fernandez, J. Gomez-Rodriguez, J. Colchero, J. Gomez-Herrero, and A. Baro, Rev. Sci. Instrum. **78**, 013705 (2007).
[39] C. Loppacher, M. Bammerlin, M. Guggisberg, S. Schär, R. Bennewitz, A. Baratoff, E. Meyer, and H. J. Güntherodt, Phys. Rev. B **62**, 16944 (2000).
[40] F. Bocquet, L. Nony, C. Loppacher, and T. Glatzel, Phys. Rev. B **78**, 035410 (2008).
[41] J. E. Sader and S. P. Jarvis, Appl. Phys. Lett. **84**, 1801 (2004).
[42] R. Hoffmann, A. Baratoff, H. J. Hug, H. R. Hidber, H. v. Löhneysen, and H.-J. Güntherodt, Nanotechnology **18**, 395503 (2007).
[43] O. H. Pakarinen, C. Barth, A. S. Foster, R. M. Nieminen, and C. R. Henry, Phys. Rev. B **73**, 235428 (2006).
[44] Y. Sugimoto, S. Innami, M. Abe, O. Custance, and S. Morita, Appl. Phys. Lett. **91**, 093120 (2007).
[45] G. H. Simon, M. Heyde, and H.-P. Rust, Nanotechnology **18**, 255503 (2007).